Simplified ONU Design in 100 Gbps C-Band PON Using Receiver-Informed Transmitter Learning

Safiya Dabwan*, Nelson Castro, Stylianos Sygletos
Aston Institute of Photonics Technologies
Aston University
Birmingham B4 7ET, United Kingdom
*sdabw20@aston.ac.uk

***Abstract*—This paper introduces a Receiver-Informed Transmitter (RITX) learning framework for point-to-multipoint passive optical networks (PONs) enabling centralised digital signal processing (DSP) at the optical line terminal (OLT), with enhanced adaptability. By shifting intelligence to the OLT, the proposed approach enables low-complexity optical network unit (ONU) operation in 100 Gb/s C-band PONs. The framework further integrates multi-task learning (MTL) to accommodate differential ONU-OLT distances and maximise service reach, yielding a twofold increase in OLT service coverage.**

***Index Terms*—passive optical network, digital signal processing, equalization, multi-task learning, machine learning, optical network unit**

I. Introduction

The growing demand for capacity in the digital era is placing increasing pressure on communication networks to support continual throughput upgrades. In last-mile access networks —predominantly passive optical networks (PONs) that connect end users to the Internet— capacity scaling is tightly constrained by stringent cost requirements. In addition, the O-band, which lies close to the zero-dispersion wavelength and has been used by most previous-generation PON systems, is becoming increasingly congested [1]. Since coexistence with legacy systems is a key requirement for PON evolution, opening the C-band for future high-capacity generations is therefore of considerable interest [2].

Deploying the C-band is particularly challenging for direct-detection (DD)–based PONs. This is because C-band transmission suffers from power fading caused by the interaction between accumulated chromatic dispersion and the square-law nature of photodetection [3]. Previous demonstrations of 100 Gb/s C-band transmission over N1-class optical distribution networks (ODNs), with losses of up to 29 dB, have therefore relied on high-complexity machine-learning algorithms at the receiver to compensate for this power fading [4]. Nevertheless, the complexity of this solution is fundamentally misaligned with the philosophy of PONs, which prioritise minimising the complexity of the optical network unit (ONU) at the user side. Consequently, alternative approaches have been sought to mitigate chromatic dispersion before the signal reaches the photodetector and is distorted by the square-law characteristics of direct detection [5]–[7]. In this direction, the authors in [5] presented a PON-compatible solution in which a pair of finite impulse response (FIR) filters pre-compensate chromatic dispersion [5]. The filters coefficients were derived from an analytical model of chromatic dispersion reported in [8]. When combined with feed-forward equalization (FFE) at the receiver, this approach enabled 64-Gb/s transmission [5]. Subsequent work has extended the concept to different wavelength bands and higher data rates, while showing that receiver-side DSP still remain important to meet performance requirements [2], [6], [10]. This work introduces a receiver-informed transmitter (RITX) learning framework in which transmitter-side filtering is adapted using feedback from the ONU. The OLT learns pre-compensation filters that capture aggregate end-to-end link impairments—rather than assuming chromatic dispersion as the only limitation—thereby eliminating the need for ONU-side digital filtering or additional processing. Building on this concept, we employ a multi-task learning (MTL) strategy [9] that enables a single optimised transmitter to simultaneously serve ONUs at different distances by expanding its coverage range.

The remainder of the paper is organised as follows. Section II introduces the proposed framework and summarises the main assumptions used in the analysis. Section III describes the simulation setup for numerical verification while Section IV presents the results and discusses them. Finally, Section V concludes this paper.

II. Proposed Approach

We follow a set of design principles aimed at a cost-effective implementation of the C-band 100 Gb/s PON. First, we leverage the inherent cost asymmetry of PONs by shifting complexity toward the OLT while keeping the ONU as simple as possible. This design choice, also adopted in prior works [5], [6], is motivated by the fact that OLT resources—and their associated costs—are shared among multiple users, whereas an ONU is required at each user's premises, which makes its cost sensitivity higher. Second, we leverage the centralised OLT DSP with optimisation capabilities that uses a feedback coming from the ONU to inform the adaptation of this DSP to maximise received signal quality. This optimisation is proven to facilitate the elimination of ONU-side DSP blocks which are typically required at conventional systems as shown in

This work was partially supported by the Royal Academy of Engineering under the Research Chairs and Senior Research Fellowships scheme.

[6]. The performance is assessed by meeting the pre-FEC BER threshold of 10^{-2} which is standardised for 50 GPON [11] and used in the research body for capacities beyond 50Gbps. The system is designed to work in two modes, training and service modes, as illustrated in Fig.1(a). The training mode occurs at least once during network setup, during which the downstream channel is occupied for configuration. It is initiated by the OLT which sends a train of pilots in the ODN and awaits feedback. In response to this pilot signal, a single or a set of ONUs respond with the distorted analogue signal received. These responding ONUs are referred to as Instructor ONUs. The received feedback is then used by the OLT to infer end-to-end channel conditions and adapt its digital shaping filters with the optimum weights which minimise the mean-square-error (MSE) against the reference pilots. The filter weights are optimised via gradient-descent backpropagation, operating on a digital twin of the transmission channel at the OLT. The choice of the number of instructor ONUs and their distance from the OLT are important discussion points that will be addressed later. In the service mode, shown in Fig.1(b), the OLT applies the trained RITX filters to shape the PAM-4 pulses, generating distortion-resilient waveforms. This channel-customised shaping ensures that the signal quality upon reception at the ONU is sufficient to achieve the target FEC BER 10^{-2}, eliminating the need for further ONU-side processing.

To validate the RITX framework, we begin by evaluating it under an idealised PON configuration in which all ONUs are uniformly separated from the OLT by 20 km, as illustrated in Fig.1(c). Under this assumption, all ONUs experience identical channel conditions, such that a single pair of transmitter filters —trained by a single instructor ONU— is sufficient to compensate for the induced distortions. This controlled setting facilitates a clear introduction of the proposed framework and enables fair comparison with alternative approaches reported in the literature. Building on the established efficacy of the RITX approach under these ideal conditions, we subsequently extend our evaluation to a more realistic scenario in which ONUs are heterogeneously distributed across the full 0–20 km range, as shown in Fig.1(d). This introduces a fundamental challenge in PON deployments that rely on centralised DSP at the transmitter as the distortions addressed by the RITX filters are dominated by chromatic dispersion, which is inherently dependent on the fibre link length. This heterogeneity introduces an over-fitting risk when training the RITX filters, particularly when the training dataset is composed of feedback from a single ONU, which may cause the filters to become overly specialised for that specific link length rather than generalising across the full 0–20 km range. Moreover, expecting a single filter pair to generalise across the full 0-20 km is an inherently unrealistic objective, given the significant variation in distortion characteristics across distances and the limited generalisation capacity of linear filters. The trade-off therefore lies in determining the optimal number of filter banks required to cover the full 0–20 km range, or at least the majority of it. This is achieved by maximising the coverage range, defined as

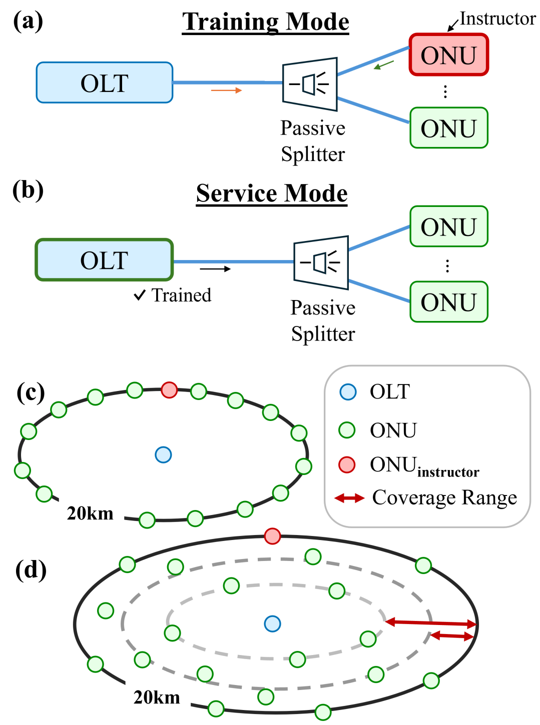

Fig. 1. (a) Training mode, in which the instructor ONU(s) transmit their response to the pilot signal they received. (b) Service mode, in which the OLT is trained and ready to serve all the ONUs within its coverage range. (c) Illustration of the assumed spatial distribution of the ONUs (green circles) around the OLT (blue circle), all being located at a uniform distance of 20 km. The Instructor ONU used to train the OLT is highlighted in red. (d) A closer-to-reality illustration of the spatial distribution of ONUs around the OLT, where the ONUs are located at varying distances within the 20 km standardised range. The red arrows denote the coverage range that the OLT is able to support depededing on its training and the number of filter banks it is using.

the span of distances that a single filter pair can reliably serve while achieving a BER at or below 10^{-2} pre-FEC. This metric is characterised by two quantities: the absolute positions of the nearest and furthest serviceable ONUs, and the width of the span between them. A wider span is desirable, as it reflects the capacity to serve a more diverse set of ONU locations with a single filter pair. To provide full coverage of the 20 km span, a filter bank architecture is employed at the transmitter, wherein each filter bank is tailored to compensate for the distortion profile of a specific sub-range of distances. The fewer filter banks required to serve the full 20 km range, the lower the resulting system complexity. Therefore, we employ multitask learning, wherein a single filter pair is trained using feedback from multiple spatially diverse ONUs to maximise their coverage range. In this study, we provide insights into the optimal selection of the number of instructor ONUs and their spatial placement.

III. Simulation Setup

The proposed framework is validated through numerical simulations based on realistic models of each building block in the system shown in Fig.2. A 100 Gbps downstream C-band link is realised using PAM-4 modulation within an in-phase/quadrature direct-detection (IQDD) architecture [5], [7]. At the OLT, an IQ Mach–Zehnder Modulator (IQ-MZM) is used to provide full-field electrical to optical modulation, hence enabling transmitter-side waveform shaping and chromatic dispersion pre-compensation— a capability that intensity modulation alone cannot offer. Although the IQ-MZM introduces greater complexity than a simple intensity modulator for a single-dimensional modulation format such as PAM-4, this is a justifiable trade-off since the added complexity is confined to the OLT, a shared network resource. The IQ-MZM's sinusoidal transfer function is modelled to subject the signal to realistic nonlinear distortion. The in-phase and quadrature arms are biased at the quadrature and null points, respectively, and the electrical drivers are configured so that the signal's real component sweeps the RF range, producing in-phase optically modulated pulses. Bandwidth limitations of the modulator are represented by a first-order Gaussian low-pass filter with a 3 dB cut-off frequency of either 18.75 GHz or 37.5 GHz, corresponding to the used optoelectronic class, whether it is 25 G or 50 G-class, respectively.

The IQ-MZM is driven by oversampled PAM-4 pulses at 2 samples per symbol (SpS), pre-distorted by complex-valued finite-impulse-response (FIR) filters. The nature of these filters differs between the two systems studied in this paper. In the RITX system, the filters are initialised by the analytical chromatic dispersion compensation model derived in [8] and subsequently adapted through training, as will be detailed later in this section. In the conventional reference system

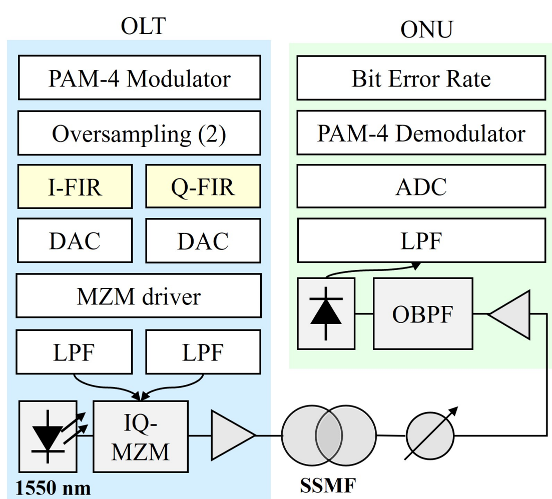

Fig. 2. The simulation setup of the PON system incorporating trainable filters at the the transmitter. LPF: low-pass filter, OBPF: optical band-pass filter

[6], the filter weights are fixed directly to Chagnon's model, assuming prior knowledge of the fibre link length and group velocity dispersion (GVD) parameter, which determines the rate of change of group velocity with frequency in ps^2/km. This prior knowledge also assists in determining the required number of taps for those filters, which according to the model in [8] are dependent on the $\beta_2 \cdot L$ factor, where L is the fibre length. In addition, the conventional system employs a pre-emphasis (PE) filter to compensate for the transmitter bandwidth roll-off, defined in the frequency domain as $P(f) = X_{des}(f)/(X_{Tx}(f) + n_0)$ where $X_{des}(f)$ and $X_{Tx}(f)$ are the desired and actual transmitter Gaussian frequency responses, and n_0 is a regularisation term [16].

Semiconductor optical amplifiers (SOAs) are deployed at both the transmitter and receiver to meet the power budget requirements imposed by the high ODN splitting losses. Both amplifiers are modelled with a noise figure of 7.5 dB and assumed to operate in the linear regime. This assumption is valid due to the low power of the signal at the input of the amplifiers. SOAs are selected for their cost-effectiveness and ease of integration, making them well-suited for future very-high-speed-PONs (VHSP) deployments [14]. The booster SOA provides a 7 dB of gain, launching 11 dBm signal power into the fibre, while the pre-amplifier SOA provides 11 dB of gain.

The optical signal propagation in the fibre is simulated by numerically solving the nonlinear Schrödinger equation (NLSE) via the symmetric split-step fourier method (SSFM), capturing chromatic dispersion, Kerr nonlinearity, and attenuation. The link operates at 1550 nm with the following fibre parameters: $D = 17\ \mathrm{ps/(nm \cdot km)}$, $\gamma = 1.3\ (\mathrm{W \cdot km})^{-1}$, and $\alpha = 0.2\ \mathrm{dB/km}$. N1-class ODN losses are introduced via an optical attenuator that imposes a 29 dB of loss.

At the receiver side, both polarisations are bandpass filtered after pre-amplification using a a fourth-order Gaussian optical bandpass filter (OBPF) to suppress out-of-band amplified spontaneous emission (ASE) noise. A square-law photodetector with responsivity of $0.7\ \mathrm{A/W}$ and IRND $15\ \mathrm{pA}/\sqrt{\mathrm{Hz}}$ then detects the signal, with shot and thermal noise modelled as Gaussian processes. Photodiode bandwidth is modelled identically to that of the modulator. DACs and ADC are assumed to be ideal with no noise contribution and a sufficiently high quantisation resolution.

After downsampling to 1 SpS, the signal is processed according to the system in use. In the RITX system, optimal demodulation of the PAM-4 signal is applied directly without further processing. In the conventional untrained system, an adaptive feed-forward equaliser (FFE) compensates for residual distortions. The required number of taps for the FFE to achieve the desired performance i.e., 10^{-2} is dependent on the system bandwidth and whether a square-root (SQRT) nonlinearity mitigation block precedes the FFE. The performance is assessed via direct error counting over 2 million simulated bits to calculate the bit error rate (BER).

The RITX filter adaptation is performed during an initial training stage during the network setup, as outlined in Section II. The transmitter makes use of a differentiable digital twin of the channel, constructed from the component equations and implemented in Tensorflow 2.6 [13]. Tensorflow enables GPU-accelerated computations of the automated gradient calculations, which enables fast and efficient implementation of learning machine functionalities. In deployments where having an accurate digital twin of the link in Tensorflow is challenging, alternatives exist, such as using a measurementbased surrogate channel model [12], or using a genetic learning algorithm as the covariance matrix adaptation evolution strategy (CMA-ES) which was used in [15] for a similar adaptation task. Training begins upon reception of the receiver feedback in response to pilots sent by the transmitter. Together, this feedback and the reference pilots constitutes the training set, compromising 4096 symbols, which is used to quantify the mean square error (MSE) against the reference pilots. The MSE is then backpropagated through the differentiable digital twin to obtain filter weight updates that minimise the error. Adam optimiser is used here to apply weight updates, employing momentum to ensure stable updates and rapid convergence, with a learning rate of 0.01. The weights update process is carried out iteratively over 100 epochs, by which the MSE converges to an error floor. For multi-task learning case, the same methodology applies, except that the training dataset size scales to 4096 symbols × number of instructor ONUs, with each ONU contributing an independent feedback block of 4096 symbols.

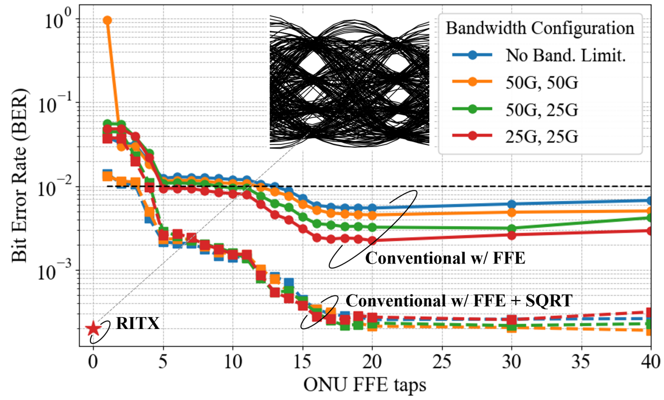

Fig. 3. Performance of the receiver-informed transmitter (RITX) system tested with 25G-class optoelectronics in an N1-class PON. The conventional system uses analytical fixed transmitter filters with adaptive FFE of varying tap counts, with and without SQRT, and requires 5–10 taps to meet the BER threshold of 10^{-2} (dashed line) depending on the bandwidth configuration and receiver type. Matching the RITX performance requires an FFE+SQRT receiver with at least 17 taps, highlighting the complexity reduction advantage of the RITX approach

IV. Results and Discussion

To evaluate the performance of the RITX system, we compare it against the conventional system which relies on untrained analytical transmitter-side filters and receiver-side equalisation described in detail in Section III. We investigate the effect of bandwidth constraints at both the transmitter and receiver by considering optoelectronics components of bandwidth specifications similar to previous PON generations limitations, specifically the 25G and 50G classes defined in Section III. Since the conventional system relies on a feed-forward equaliser (FFE) at the receiver, we systematically vary the number of FFE taps across both conventional systems used for benchmarking: one that incorporates a SQRT function prior to the FFE for nonlinearity mitigation and another that omits it. Referring to the results presented in Fig 3, the RITX filters achieve performance equivalent to that of the conventional system operating with a minimum of 17 FFE taps in conjunction with the usage of SQRT function, under the most bandwidth-constrained scenario (25G-class transmitter and 25G-class receiver) without requiring any FFE taps at the receiver. This result demonstrates the effectiveness of the trained transmitter approach in migrating signal-processing complexity from the receiver to the transmitter, thereby reducing ONU complexity and associated system cost. Furthermore, the results clearly illustrate the substantial benefit of incorporating the SQRT function in the conventional system, which markedly reduces the number of FFE taps required to attain the target BER threshold and enables performance levels that would otherwise remain unachievable. Finally, no significant performance differentiation is observed across the explored optoelectronic bandwidth classes, suggesting that bandwidth limitation is not the dominant source of distortion in the system, and that the linear filters employed are compensating for it adequately.

To examine the coverage range of RITX filters trained with a single instructor ONU, we position the instructor at different locations within the 0-20 km range, perform training, and evaluate the BER across the full 0-20 km span. By recording the distances at which the 10^{-2} BER threshold is achieved, we obtain the coverage ranges presented in Fig. 4(a). Each stem in Fig.4(a) represents a distinct filter bank trained with feedback from an ONU positioned at different distances. An average coverage range of 5 km is observed across all filter banks. From Fig.4(a), we conclude that serving ONUs across 2-20 km range requires 4 filter banks, each trained with a single instructor ONU located at 2, 10, 14, and 20 km. We, subsequently, extend our investigation to explore how training with multiple ONUs of increasing spatial separation influences the filter coverage range. Fig.4(b) presents two groups of filter banks centred around 10 and 20 km, each serving different ONU population. It is evident that there is a general tendency for the coverage range to increase with the spatial variance among instructor ONUs. However, performance degrades once the spatial separation between instructor ONUs exceeds 10 km. The orange filter banks shown in Fig.4(b) centred around 10 km are able to achieve the widest coverage range when trained with 3 instructor ONUs positioned at 5, 10 and 15 km. Multitask learning extends the coverage of a single-task filter trained with feedback from an ONU at 10 km (marked with orange arrow in Fig.4(a)) from 4 to 8 km, as demonstrated by the orange box in Fig.4(b)), with edges at 5 and 10 km. The same consistent results are observed for the filter banks centred around 20 km, where training with ONUs at 15, 20, and 25 km yields the widest coverage range, spanning from 15 to 23 km. This 8 km span represents an improvement over the 5 km coverage range obtained when training with feedback from a single ONU at 20 km. To thoroughly examine the benefit of multitask learning, the effect of increasing the number of instructor ONUs within an identical spatial variance is evaluated for 3 and 5 ONUs. The results presented in Fig.4(c)) indicate that when the spatial variance between the instructor ONUs remains within the optimal limit of 10 km, increasing

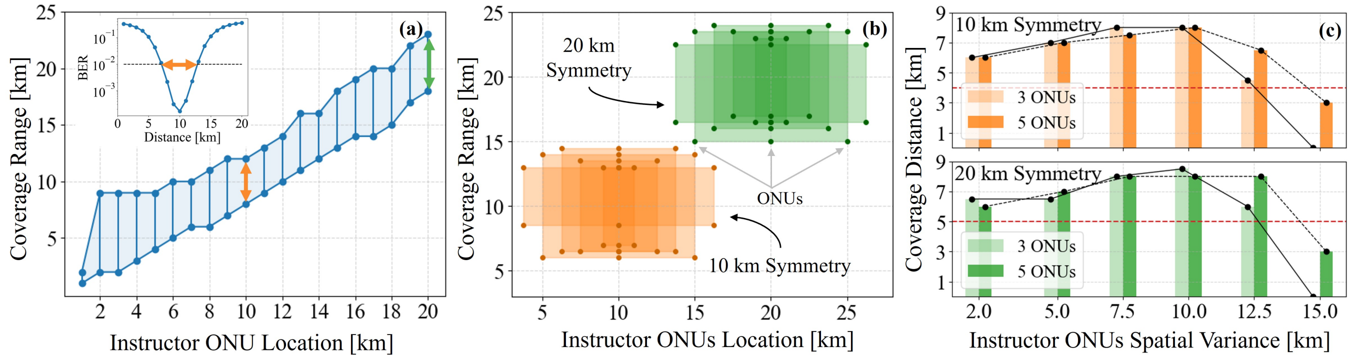

Fig. 4. (a) The coverage range achievable by the OLT when trained using a single instructor ONU at the indicated location. An average coverage of 5 km per filter bank is achieved, implying that 4 filter banks are required to serve the 2–20 km range. The inset illustrates how the coverage range is determined for a filter bank trained with an instructor ONU at 10 km. (b) The coverage range achieved when training with 3 instructor ONUs, whose positions are marked with dots. Two filter bank configurations are explored, with instructor ONUs placed symmetrically around 10 km and 20 km. Increasing the spatial separation between instructor ONUs broadens the coverage range until 10 km. (c) The effect of increasing the number of instructor ONUs on the coverage range, for different spatial separations. Increasing the number of instructor ONUs does not yield tangible benefits

the number of instructor ONUs yields no additional benefit. Beyond this limit, however, an improvement is observed, albeit alongside a general degradation in overall coverage range.

V. Conclusion

This work proposes and demonstrates the receiver-informed transmitter (RITX) framework for point-to-multipoint PONs, enabling low-complexity ONUs, achieving reductions in overall network cost and footprint. Using the proposed RITX approach, the need for a 17-tap feed-forward equaliser (FFE) and a square-root (SQRT) operation at the ONU is eliminated. Moreover, by leveraging multi-task learning, OLT trained filters are able to support ONUs across double the distance range that could be achieved by single-ONU training. To the best of our knowledge, this represents the simplest ONU design reported for a 100 Gb/s, 29 dB C-band PON.

Acknowledgment

The authors thank Wladek Forysiak and Ian Phillips for constructive discussions. Language editing assistance was provided by Claude.

References

[1] P. Torres-Ferrera and F. Effenberger and M. S. Faruk and S. J. Savory and R. Gaudino, “Overview of High-Speed TDM-PON beyond 50 Gbps per Wavelength Using Digital Signal Processing [Invited Tutorial],” J. Opt. Commun. Netw., vol. 14, no. 12, pp. 982, Dec. 2022, doi: 10.1364/JOCN.468920

[2] H. Wang and P. Torres-Ferrera and G. Rizzelli and R. Mercinelli and V. Ferrero and R. Gaudino, ”200 Gbps/λ PON Downstream C-Band Direct-Detection Links with 29 dB Power Budget,” Applied Sciences, vol. 12, no. 7, pp. 3538, Mar. 2022, doi: 10.3390/app12073538

[3] Y. Zhu *et al.*, “Comparative study of cost-effective coherent and direct detection schemes for 100 Gb/s/λ PON,” J. Opt. Commun. Netw., vol. 12, no. 9, pp. D36–D47, 2020, doi: 10.1364/JOCN.390911.

[4] L. Yi *et al.*, “Machine learning for 100 Gb/s/λ passive optical network,” J. Lightw. Technol., vol. 37, no. 6, pp. 1621–1630, Mar. 2019, (Invited Paper), doi: 10.1109/JLT.2018.2888547.

[5] J. Zhang *et al.*, “64 Gb/s/λ downstream transmission for PAM-4 TDM-PON with centralized DSP and 10G low-complexity receiver in C-band,” in Proc. Eur. Conf. Opt. Commun. (ECOC), 2017, pp. 1–3, doi: 10.1109/ECOC.2017.8346007.

[6] P. Torres-Ferrera *et al.*, “Experimental demonstration of 100 Gbps/λ C-band direct-detection downstream PON using non-linear and CD compensation with 29 dB+ OPL over 0 km–100 km,” J. Lightw. Technol., vol. 40, no. 2, pp. 547–556, 2022, doi: 10.1109/JLT.2021.3129446.

[7] H. Wang *et al.*, “100 Gbps/λ C-band CD digital pre-compensated and direct-detection links with simple non-linear compensation,” IEEE Photon. J., vol. 13, no. 4, pp. 1–8, 2021, doi: 10.1109/JPHOT.2021.3107487.

[8] M. Chagnon, “Optical communications for short reach,” *Journal of Lightwave Technology*, vol. 37, no. 8, pp. 1779–1797, Apr. 2019, doi: 10.1109/JLT.2019.2901201.

[9] R. Caruana, “Multitask learning,” in Learning to Learn, S. Thrun and L. Pratt, Eds. Springer US, 1998, pp. 95–133, doi: 10.1007/978-1-4615-5529-2_5.

[10] P. Torres-Ferrera, V. Ferrero, and R. Gaudino, “100 Gbps PON L-band downstream transmission using IQ-MZM CD digital pre-compensation and DD ONU receiver,” in Opt. Fiber Commun. Conf. (OFC) 2020, pp. Th1B.1, doi: 10.1364/OFC.2020.Th1B.1.

[11] D. Zhang and D. Liu and X. Wu and D. Nesset, ”Progress of ITU-T higher speed passive optical network (50G-PON) standardization,”J. Opt. Commun. Netw. vol. 12, no. 10, pp.D99, Oct. doi: 2020, 10.1364/JOCN.391830

[12] S. Hernandez, C. Peucheret, F. Da Ros, and D. Zibar, “Experimental demonstration of end-to-end optimization for directly modulated laser-based IM/DD systems,” in Opt. Fiber Commun. Conf. (OFC) 2025, 2025, pp. W4H.3, doi: 10.1364/OFC.2025.W4H.3.

[13] M. Abadi et al., “TensorFlow: Large-Scale Machine Learning on Heterogeneous Systems,” Software, 2015. [Online]. Available: https://www.tensorflow.org

[14] R. Bonk, “SOA for future PONs,” in *Optical Fiber Communication Conference (OFC)*, OSA Technical Digest, Optica Publishing Group, 2018, paper Tu2B.4.

[15] S. Masaad *et al.*, “Experimental Demonstration of 4-Port Photonic Reservoir Computing for Equalization of 4 and 16 QAM Signals,” *J. Lightwave Technol.*, vol. 42, no. 24, pp. 8555–8563, Dec. 2024, doi: 10.1109/JLT.2024.3444480.

[16] A. Napoli *et al.*, “Digital Compensation of Bandwidth Limitations for High-Speed DACs and ADCs,” *J. Lightwave Technol.*, vol. 34, no. 13, pp. 3053–3064, 2016, doi: 10.1109/JLT.2016.2519260.